Ultralong Organic Phosphorescence in the Solid State: the Case of Triphenylene Cocrystals with Halo- and Dihalo-penta/tetrafluorobenzene

Simone d'Agostino,[a] Floriana Spinelli,[a] Paola Taddei,[b] Barbara Ventura[c] and Fabrizia Grepioni*[a]*

[a] Dipartimento di Chimica "Giacomo Ciamician", Università di Bologna, Via F. Selmi, 2, 40126 Bologna, Italy.

[b] Dipartimento di Scienze Biomediche e Neuromotorie, Università di Bologna, Via Belmeloro 8/2, 40126 Bologna, Italy.

[c] Istituto ISOF-CNR, Via P. Gobetti, 101, 40219 Bologna, Italy.

ABSTRACT

The polycyclic aromatic hydrocarbon (PAH) triphenylene (TP) has been reacted with halo-pentafluorobenzene (XF5, X = Br, I) and 1,4-dihalo-tetrafluorobenzene (X2F4, X = Br, I) to yield the corresponding cocrystals TP·BrF5, TP·Br2F4, TP·IF5, and TP·I2F4 form I. These materials have been synthesized by dissolving TP into an excess of liquid or molten co-former, and single crystals have been grown via seeding chloroform solutions. They have been fully characterized by a combination of techniques including X-ray diffraction, Raman, and luminescence spectroscopy in the solid state. TP·I2F4 form I was found to undergo a single-crystal to single-crystal (SCSC) polymorphic phase transition induced by temperature (when cooled down to 100K) leading to the new form TP·I2F4 form II, which is transformed back into the first structure when brought again at

RT. This behavior was confirmed also by Raman spectroscopy. Upon cocrystallization and as a result of the external heavy atom effect, all crystalline materials exhibited bright room temperature phosphorescence clearly visible by naked eye. The latter was almost exclusive for cocrystal TP·I2F4, whereas for TP·Br2F4 both fluorescence and phosphorescence were detected. In TP·Br2F4, the phosphorescence lifetime was of the order of 200 ms, and with the visual outcome of an orange phosphorescence lasting for a couple of seconds upon ceasing the excitation, that makes this compound classifiable as an Ultralong Organic Phosphorescent (UOP) material. The results evidenced the role of the nature of the heavy atom in governing the phosphorescence output from organic cocrystals.

INTRODUCTION

Solid luminescent materials constitute an attractive field of research, not only from a theoretical point of view, but also because of their potential applications in the development of optoelectronic devices. In contrast to the extensive number of examples of metal-based organometallic phosphors, purely organic materials that display room temperature phosphorescence (RTP) are still quite rare.[1-6]

Even more rare is the phenomenon of the so-called Ultralong Organic Phosphorescence (UOP), namely persistent luminescence, which lasts for a long time (up to hours) after the excitation source has been switched off,[7,8] especially when occurring in the visible range. As a definition, a material can be considered an UOP emitter when its luminescence lifetime is longer than 100 ms.[4]

Recently it has been reported for polymers,[9,10] host-guest systems,[11-13] carbon dots dispersed into polymeric matrices,[14] self-assembled supramolecular frameworks or H-aggregates[15] as well as in single-component small molecules like iminodibenzyl[16] and carbazol-derivatives based crystalline materials.[17]

In the specific, persistent RTP has received considerable attention in the last decade due to significant advantages and potential over fluorescence for application in bioelectronic and optoelectronic devices.[18-20] Phosphorescence, indeed, may enable highly sensitive bioimaging because of the exclusion of background and endogenous fluorescence, and active layers based on phosphorescent materials have shown a quantum efficiency up to 3-fold higher with respect to fluorescent ones in OLED devices.

Crystal engineering,[21-23] which has as ultimate goal the tailoring of physical and chemical properties of solids through the study and exploitation of intermolecular interactions within the context of the crystal packing, offers the powerful tool of cocrystallization for designing of materials with desirable properties.

Organic cocrystals are multi-component systems wherein a molecule of interest and a co-former, purposely chosen to alter the packing of the former, self-assemble together within a unique crystalline structure through non-covalent interactions. Though simple, this approach[24] has proved to be a successful tool for achieving optical properties of use for several applications, such as NIR photothermal conversion,[25] white-light emission,[26] development of thermo- and photochromic materials,[27-29] fluorescence color modification[29-32] and enhancement[33,34] as well as for promoting delayed-fluorescence[35-37] and room temperature phosphorescence from purely organic systems.[38-41]

The purpose of this study is to design and investigate organic cocrystals that could display phosphorescence in the solid state and at RT. This approach is based on a strategy that relies on cocrystal formation via π-hole$\cdots$π interactions[37,42]and halogen bond (XB) of the kind X$\cdots$π[43-45] and makes use of organic co-formers containing heavy atoms (halo-perfluorobenzene). These play two key roles within the cocrystals: (i) they serve as solid diluents to prevent the emitting molecule from aggregating or self-quenching, and (ii) they act as perturbants, inducing phosphorescence emission in the emitting chromophore. In particular, our study focuses on the investigation of the role of the

halogen involved in cocrystal formation in tuning the optical properties of the organic photoactive component, by using both iodide- and bromide-containing co-formers.

Triphenylene (TP) has been chosen as the photoactive component given its interesting luminescence features[46-48] and it has been cocrystallized with the bromo-pentafluorobenzene (BrF5), iodo-pentafluorobenzene (IF5), 1,4-dibromo-tetrafluorobenzene (Br2F4), and 1,4-diiodo-tetrafluorobenzene (I2F4) (see Scheme 1). Cocrystals were obtained as polycrystalline samples through mechanochemical synthesis and from the melt, while single crystals have been successfully grown by seeding the so-obtained materials. The solid state characterization was carried out through a combination of XRD techniques, Raman, and luminescence spectroscopy.

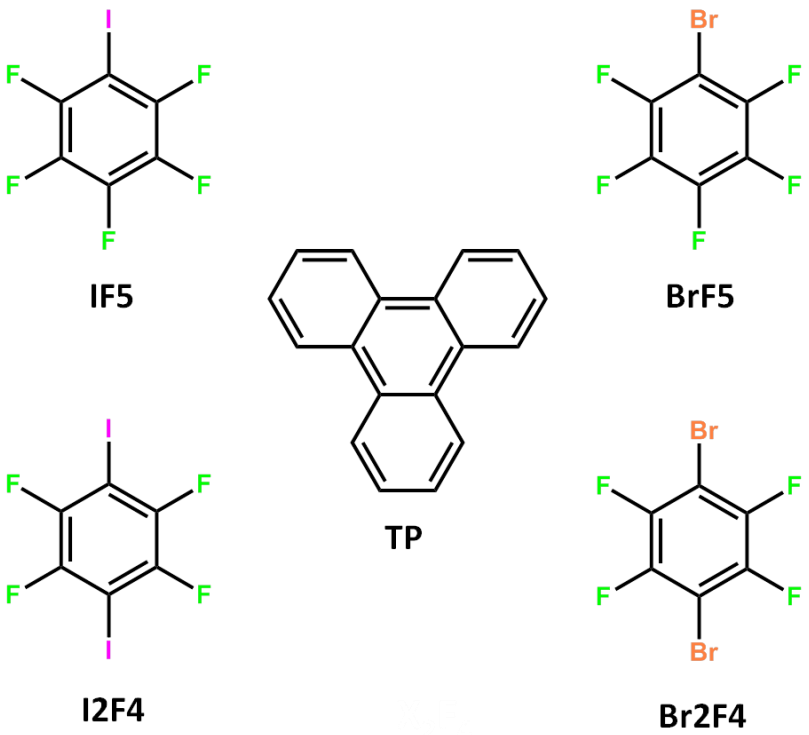

Scheme 1. Molecular structure of the chosen building blocks.

EXPERIMENTAL SECTION

Synthesis

All reagents were purchased from Sigma-Aldrich and recrystallized from ethanol (EtOH) prior to use.

TP·XF5: 50 mg (0.22 mmol) of triphenylene (TP) were suspended in 1 mL of liquid of the co-former bromopentafluorobenzene (BrF5) or iodopentafluorobenzene (IF5) and warmed gently, in a closed vial, until a clear solution was obtained. Diffraction quality single crystals were obtained by slow cooling of the solutions to RT.

TP·X2F4: 100 mg (0.44 mmol) of triphenylene (TP) were manually ground with 2 equivalents of the co-former 1,4-dibromo-tetrafluorobenzene (Br2F4), 260 mg, or 1,4-diiodo-tetrafluorobenzene (I2F4), 350 mg, and then placed in a closed vial and warmed gently in an oil bath until complete dissolution of TP into molten co-formers (Br2F4 m.p = 81°C and I2F4 m.p. = 110°C). The resulting solutions were kept warm for 1 hour and then left to slowly cool down to RT. Diffraction quality single crystals were obtained by slow evaporation at RT of chloroform solution seeded with the desired crystal phase.

X-ray Diffraction

Single crystal data for all cocrystals were collected at 100K, except TP·I2F4 which was collected either at 100 K and RT (300 K), on an Oxford XCalibur S CCD diffractometer equipped with a graphite monochromator (Mo-Kα radiation, λ = 0.71073Å). Data collection and refinement details are listed in Table 1. All non-hydrogen atoms were refined anisotropically. Single crystals of the co-former Br2F4 were also obtained and its structure redetermined.[49] For this compound, crystal structure and data and details are reported in Figure SI-1, and Table SI-1. For TP·BrF5 and TP·IF5,

the halo-pentafluorobenzene co-former was found to be disordered over two positions (see Figure SI-2) and refined anisotropically applying EADP constraints.

Site occupancy factors (SOFs) were also refined by adding a second free variable in the FVAR command line. Two twin unit cells were indexed for TP·I2F4 form II, and the reflection data were integrated with the default configuration for twinned crystals of CrysAlisPro software. Subsequent structure solution and refinement were performed using the HKLF4 file containing non-overlapped reflections. H_{CH} atoms for all compounds were added in calculated positions and refined riding on their respective carbon atoms. SHELX97[50] was used for structure solution and refinement on F2. The program Mercury[51] was used to calculate intermolecular interactions and for molecular graphics. Crystal data can be obtained free of charge via www.ccdc.cam.ac.uk/conts/retrieving.html (or from the Cambridge Crystallographic Data Centre, 12 Union Road, Cambridge CB21EZ, UK; fax: (+44)1223-336-033; or e-mail: deposit@ccdc.cam.ac.uk). CCDC numbers 1856795-1856800.

For ϕ-Scan experiments a fresh single crystal specimen of the cocrystal TP·I2F4 form I was selected and mounted on the diffractometer. Goniometer angles (θ, k, ω, ϕ) were set at 0° and detector distance at 45 mm, then ϕ was moved of 1° during the exposure time (20 seconds). Unit cell determinations at RT and 100 K were performed, and corresponded to those of cocrystals TP·I2F4 form I and form II, respectively.

For phase identification and Rietveld refinement purposes X-ray powder diffractograms in the 2θ range 3–70° (step size, 0.026°; time/step, 200s; 0.02 rad soller; V x A 40 × 40) were collected on a Panalytical X'Pert PRO automated diffractometer operated in transmission mode (capillary spinner) and equipped with a Pixel detector. The program Mercury[51] was used for simulation of X-ray powder patterns on the basis of single crystal data. Chemical and structural identity between bulk materials and single crystals was always verified by comparing experimental and simulated powder diffraction patterns. Powder diffraction data were analyzed with the software TOPAS4.1.[51] A shifted Chebyshev function with 7 parameters and a Pseudo–Voigt function (TCHZ type) were used

to fit background and peak shape, respectively. A spherical harmonics model was used to describe the preferred orientation. See the Supporting Information for the difference patterns and the corresponding merit figures.

Table 1. Crystal data and refinement details for crystalline TP·BrF5, TP·Br2F4, TP·IF5, and TP·I2F4 form I and form II.

	TP·BrF5	**TP·IF5**	**TP·Br2F4**	**TP·I2F4 form I**	**TP·I2F4 form II**
Formula	$C_{24}H_{12}BrF_5$	$C_{24}H_{12}F_5I$	$C_{24}H_{12}Br_2F_4$	$C_{24}H_{12}F_4I_2$	$C_{24}H_{12}F_4I_2$
fw	475.25	522.24	536.16	630.14	630.14
Temperature (K)	100	100	100	RT	100
Cryst. System	Orthorhombic	Orthorhombic	Orthorhombic	Orthorhombic	Monoclinic
Space group	$P2_12_12_1$	$P2_12_12_1$	*Pnma*	*Pnma*	$P2_1/n$
Z	4	4	4	4	4
a (Å)	7.288(1)	7.441(4)	18.167(1)	18.608(1)	7.910(5)
b (Å)	14.476(3)	14.377(7)	14.516(3)	14.582(1)	18.337(5)
c (Å)	17.385(3)	17.574(7)	7.368(6)	7.869(4)	14.423(5)
α (deg)	90	90	90	90	90
β (deg)	90	90	90	90	100.369(5)
γ (deg)	90	90	90	90	90
V (Å^3)	1834.32(6)	1880.3(1)	1943.3(5)	2135.4(3)	2057.9(1)
Dcalc (g/cm^3)	1.721	1.845	1.833	1.960	2.0134
μ (mm^{-1})	2.299	1.760	4.217	2.988	3.100
Measd reflns	29124	9473	8363	5034	6531
Indep reflns	4527	4104	1780	1954	3003
R_1[on F02, I>2σ(I)]	0.0374	0.0603	0.0514	0.0472	0.0600
wR_2 (all data)	0.0725	0.1211	0.1417	0.1050	0.2552

Raman Spectroscopy

Raman spectra were recorded on a Bruker MultiRam FT-Raman spectrometer equipped with a cooled Ge-diode detector. The excitation source was a Nd^{3+}-YAG laser (1064 nm) in the backscattering (180°) configuration. The focused laser beam diameter was about 100 μm and the spectral resolution 4 cm^{-1}. The reported spectra were recorded with a laser power at the sample of about 20 mW.

Optical Spectroscopy

Room temperature measurements were performed on powder samples placed inside two quartz slides or on single crystals placed on the top of a quartz slide. For 77 K determinations the samples were placed inside quartz capillary tubes and immersed in liquid nitrogen in a homemade quartz Dewar. Reflectance spectra were acquired with a PerkinElmer Lambda 950 UV/Vis/NIR spectrophotometer equipped with a 100 mm integrating sphere and converted in absorption spectra using the Kubelka–Munk function.[33]

A thin layer of powder was used (absorbance values below 0.2) for luminescence measurements.

Emission spectra were collected in front-face mode with an Edinburgh FLS920 fluorimeter equipped with a Peltier-cooled Hamamatsu R928 PMT (200−850 nm) and corrected for the wavelength dependent phototube response. Absolute emission quantum yields were determined according to the method reported by Ishida et al.,[53] each measurement was repeated 3 times. The limit of detection of the system is 0.020.

Gated emission spectra were acquired in front-face mode with the same fluorimeter by using a time-gated spectral scanning mode and a μF920H Xenon flash lamp (pulse width < 2 μs, repetition rate between 0.1 and 100 Hz) as excitation source. Spectra were corrected for the wavelength dependent

phototube response. Phosphorescence decays were acquired with the same apparatus in multichannel scaling mode.

Fluorescence lifetimes were measured by using an IBH time-correlated single-photon counting (TCSPC) apparatus by using a pulsed NanoLED excitation source at 331 nm. Analysis of the luminescence decay profiles against time was accomplished with the Decay Analysis Software DAS6 provided by the manufacturer. Estimated errors are 10% on lifetimes and 2 nm on emission and absorption peaks.

RESULTS AND DISCUSSION

Structural Description and Synthesis of Polycrystalline Samples

Single crystal XRD analysis for all cocrystals had to be carried out at low temperature (100K) because all samples suffered degradation under the X-ray beam except TP·I2F4 formI, for which it was possible to collect an additional dataset at RT. Interestingly, TP·I2F4 form I was found to undergo a phase transition upon cooling (see below) to a new polymorph denoted as TP·I2F4 form II.

The crystal structures of TP·BrF5, TP·IF5, TP·Br2F4, TP·I2F4 form I and II show some common features and differences. Extended stacks in which molecules of TP alternate with the corresponding halo-perfluorobenzene in an ⋯A⋯B⋯A⋯B⋯ fashion characterize all cocrystals, see Figure 1 and Table SI-2 for geometrical parameters. However, as a consequence of the different nature of the co-formers, the inter-planar distances and tilted angles between the triphenylene and the halo-perfluorobenzene are slightly different (Table SI-2).

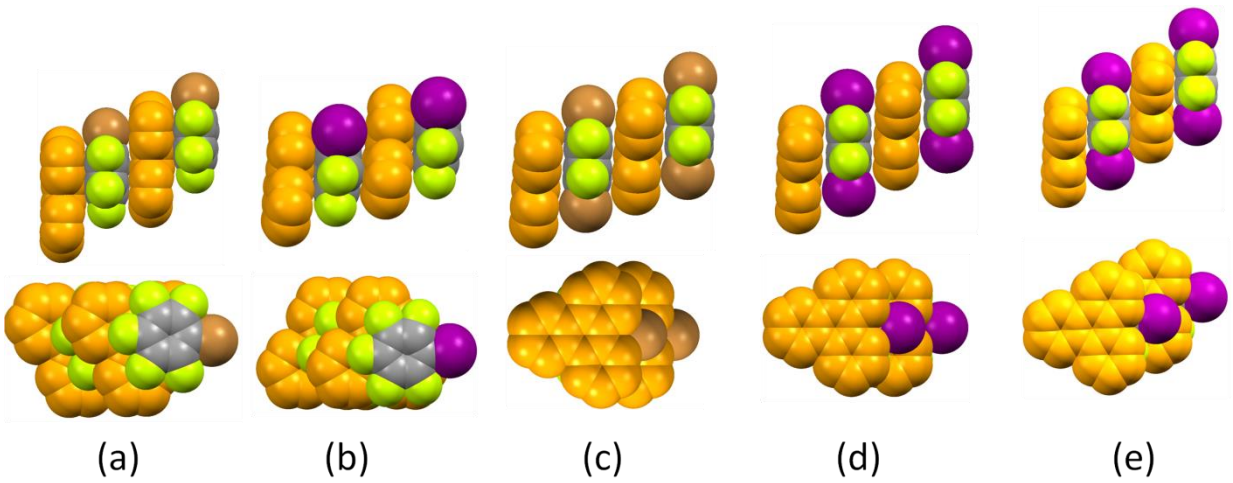

Figure 1. Side and top views of the columnar stacking found in cocrystals: (a) TP·BrF5, (b) TP·IF5, (c) TP·Br2F4, (d) TP·I2F4 form I and (e) TP·I2F4 form II. TP molecules in orange. H_{CH} omitted for clarity.

As shown in Figure 2, TP·Br2F4 and TP·I2F4 form I and II cocrystals are further stabilized by weak X···X interactions of type II[54,55] since the interatomic distances are significantly shorter than the respective sum of the van der Waals radii of the X-atoms involved[56,57] (3.70 Å for X = Br and 3.96 Å for X = I) as well as by weak halogen bonding interactions of the kind X···π,[43,44]see Table SI-2. These X··· π intermolecular interactions can be seen as a particular case of directional halogen bonding where the electron depleted polar regions of the polarized halogens reach out toward the electron-rich π-orbitals of an aromatic compound.

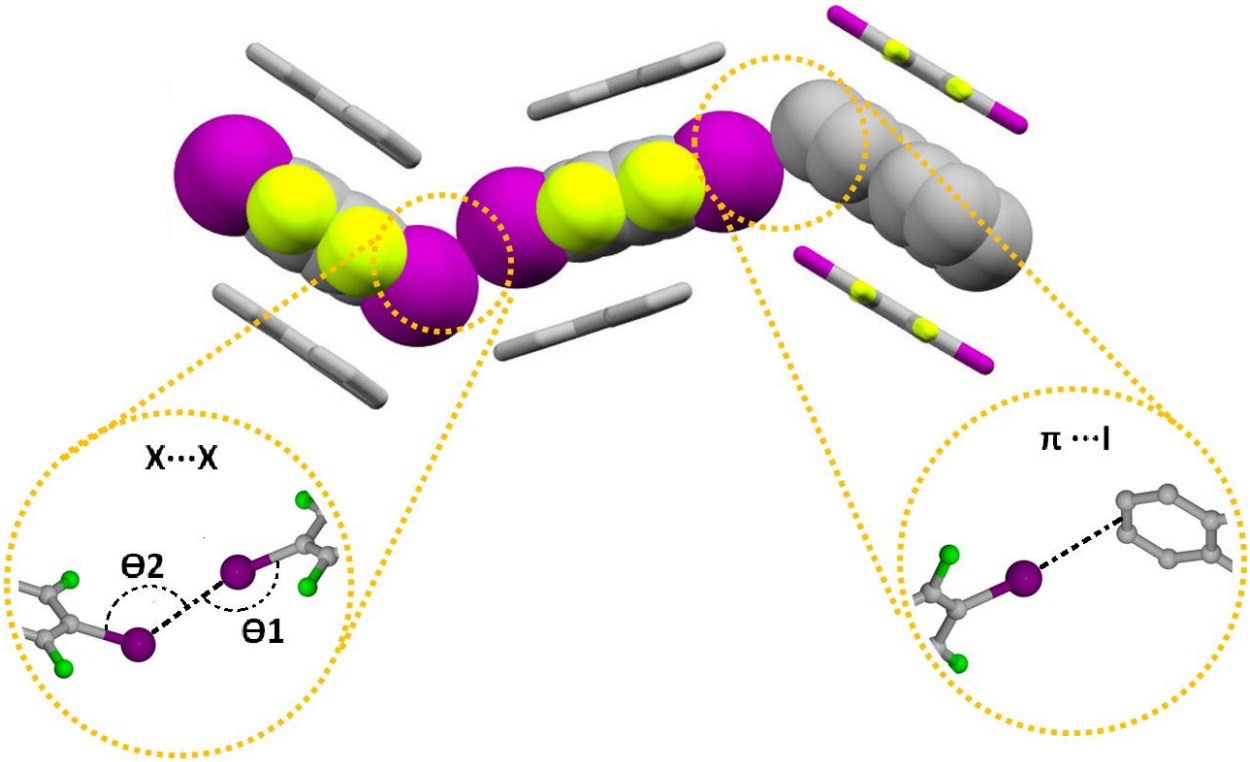

Figure 2. The weak halogen bonds X···X interactions of type II and X··· π detected within TP·X2F4 cocrystals. H_{CH} omitted for clarity. See Table SI-2 for geometrical parameters.

Upon cooling to 100 K, TP·I2F4 form I undergoes a SCSC phase transition into a new form, viz. TP·I2F4 form II. Veridicity of the SCSC transition was confirmed by recording ϕ-scans diffraction patterns for each step of a cooling-heating cycle (Figure SI-3). The two polymorphs display a different unit cell, see Table 1. In form II the components show a difference in their reciprocal orientation, with the I2F4 molecule slightly shifted with respect of the TP (Figures 1 and 3).

Cocrystal TP·I2F4 form II is, in turn, transformed back into form I when brought again at RT, i.e. the RT ⇄ LT transformation is reversible. Thus, this system is enantiotropic.[57]

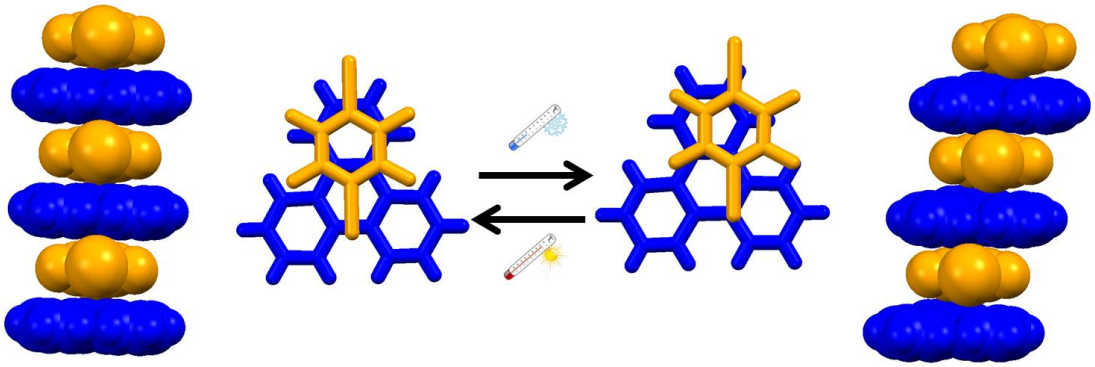

Figure 3. Representation of the reversible transformation between TP·I2F4 form I and form II triggered by the thermal stimulus.

Considering that the π-hole···π interactions supply a "milder external heavy atom effect"[37,42] we expected to quench TP fluorescence more than its phosphorescence, achieving thus UOP from TP-based cocrystals. Cocrystallization results in bright RT phosphorescence, clearly visible at naked eye, which lasts for a few seconds after removing the excitation light source (see Figure 4 and a video in the Supporting Information).

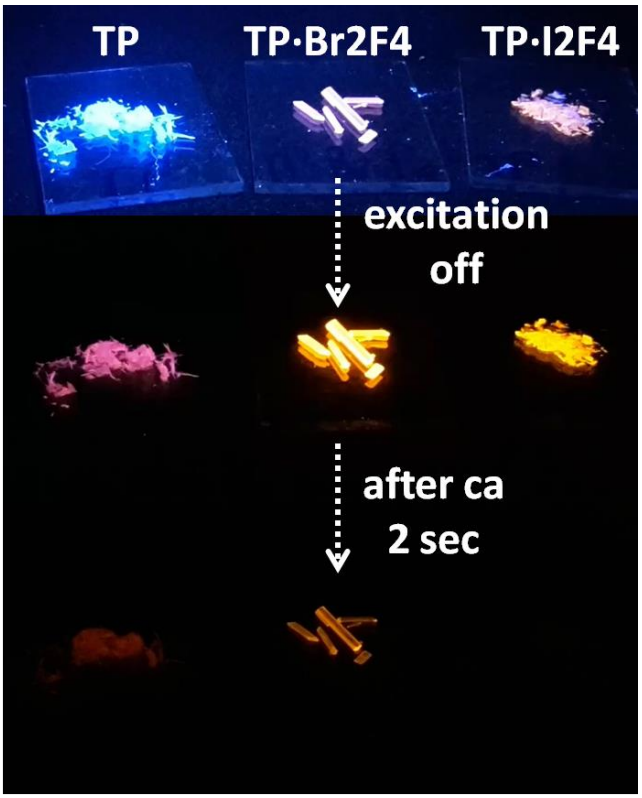

Figure 4. Photographs of TP (left), TP·Br2F4 (~~left~~ center) and TP·I2F4 form I (right) crystals taken under 365 nm UV light and after ceasing the UV irradiation.

Production of bulk polycrystalline samples stable and as pure as possible is crucial to perform reliable spectroscopic characterization in the solid state. Unfortunately, cocrystals TP·BrF5 and TP·IF5, when taken out of their mother liquors, rapidly degrade because of the loss of the co-former, leaving thus polycrystalline samples of TP. For them further spectroscopic studies could not be carried on.

We, therefore, focused our efforts in preparing pure polycrystalline samples of the cocrystals TP·Br2F4 and TP·I2F4 form I, both by solution methods and mechanochemistry. Unfortunately, in each case reactions were never quantitative, since the polycrystalline powders were found to contain a mixture of reactants (TP and X2F4) and cocrystal, making thus the resulting solids unsuitable for further spectroscopic and photophysical characterization. For example, in the ball-milling synthesis of TP·Br2F4, it was not possible to obtain reaction completeness either starting from a 1:1

stoichiometric ratio of reagents, or when a large excess of co-formers was used (ratio of 1:2) and milling frequency and time increased (up to 90 minutes at 20Hz), see Figure SI-4.

To circumvent these drawbacks, we decided to attempt the synthesis of cocrystals TP·Br2F4 and TP·I2F4 form I from the melt. However, even this approach showed some critical points. Due to the sublimation of the co-formers, we had to start from an excess of X2F4 to achieve complete conversion of TP into the corresponding cocrystal (Figure SI-5). The so-obtained samples were then used for the spectroscopic and photophysical characterization (vide infra). Scheme 2 depicts a comparison between the different synthetic strategies.

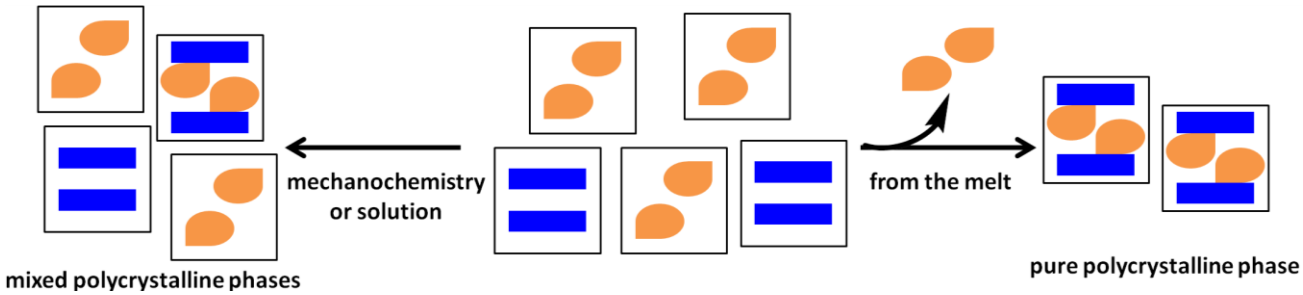

Scheme 2. Comparison between different synthetic approaches highlighting why cocrystallization from the melt is more effective for the obtainment of polycrystalline samples suitable for spectroscopic analyses.

Raman Spectroscopy

The spectrum of the TP·I2F4 form I cocrystal (Figure 5) was dominated by the bands of TP, although the bands of I2F4 were clearly visible and identified. Wavenumbers and assignments[58-61] of the main Raman bands of the cocrystal, TP and I2F4 are reported in Table SI-3.

Going from the co-formers to the cocrystal, several bands underwent wavenumber shifts and changes in relative intensities, as shown in Figure 5 and Table SI-3. In particular, the band observed at 159 cm^{-1} in I2F4 (assignable to C-I stretching + ring elongation[58]) shifted to 163 cm^{-1} in the cocrystal, i.e. to a higher wavenumber value. An analogous trend has been reported by other authors

for cocrystals constructed by I2F4 and polyaromatic hydrocarbons based on C-I···π halogen bonding and other assisting weak interactions.[38,41,64,65]

Many TP bands shifted upon adduct formation; the blue shift observed for the TP C-H stretching band at 3051 cm^{-1} (which shifted to 3056 cm^{-1} in the cocrystal) was reported also by Shen et al.[65] for the cocrystals of I2F4 with naphthalene or phenantrene. The red shift of the TP C-H in plane bending at 1247 cm^{-1} (which shifted to 1245 cm^{-1} in the cocrystal) was observed also for I2F4-pyrene cocrystals.[64]

These changes as well as the other observable in Figure 5 (and detailed in Table SI-3) may be assigned to the intermolecular interactions between I2F4 and TP; actually, as can be easily seen in Figure SI-8, the spectrum of the cocrystal was significantly different from the sum of the spectra of the two components. The main differences between the experimental spectrum and the theoretical one were observed in the TP aromatic C-H and C-C stretching, C-H in plane and out of plane bending, ring deformation and lattice vibrations regions. These findings suggest that the interaction with I2F4 determined structural rearrangements into the TP co-former. It is interesting to note that in the theoretical spectrum, several bands assignable to I2F4, i.e. those at 1384, 442, 404 and 334 cm^{-1} (indicated with an asterisk) appeared with higher intensity than in the experimental spectrum. This result is in agreement with the literature,[38,41] which reports a weakening of the above mentioned bands upon cocrystal formation. On the other hand, the I2F4 bands at 308 and 159 cm^{-1} were stronger in the experimental spectrum than in the theoretical one, the latter to a significant extent, confirming to be the main marker band to detect the halogen bond occurrence.

The low-wavenumber range appeared the most suitable to confirm the occurrence of the reversible polymorphic transformation of TP·I2F4 form I into its form II upon cooling to 77 K. As can be seen from the spectra reported in Figure SI-9, the two polymorphs appeared significantly different both for the wavenumber position of the above mentioned C-I stretching + ring elongation mode (163 and 161 cm^{-1} in forms I and II, respectively), as well as for the spectral range below, where lattice

vibrations fall. Upon cooling, a band at 129 cm^{-1} appeared and significant band wavenumber shifts and changes in relative intensities were observed below 100 cm^{-1}. The spectral changes induced by cooling (which appeared reversible upon heating to RT) are consistent with the formation of a new polymorph characterized by different halogen bonding and molecular packing.

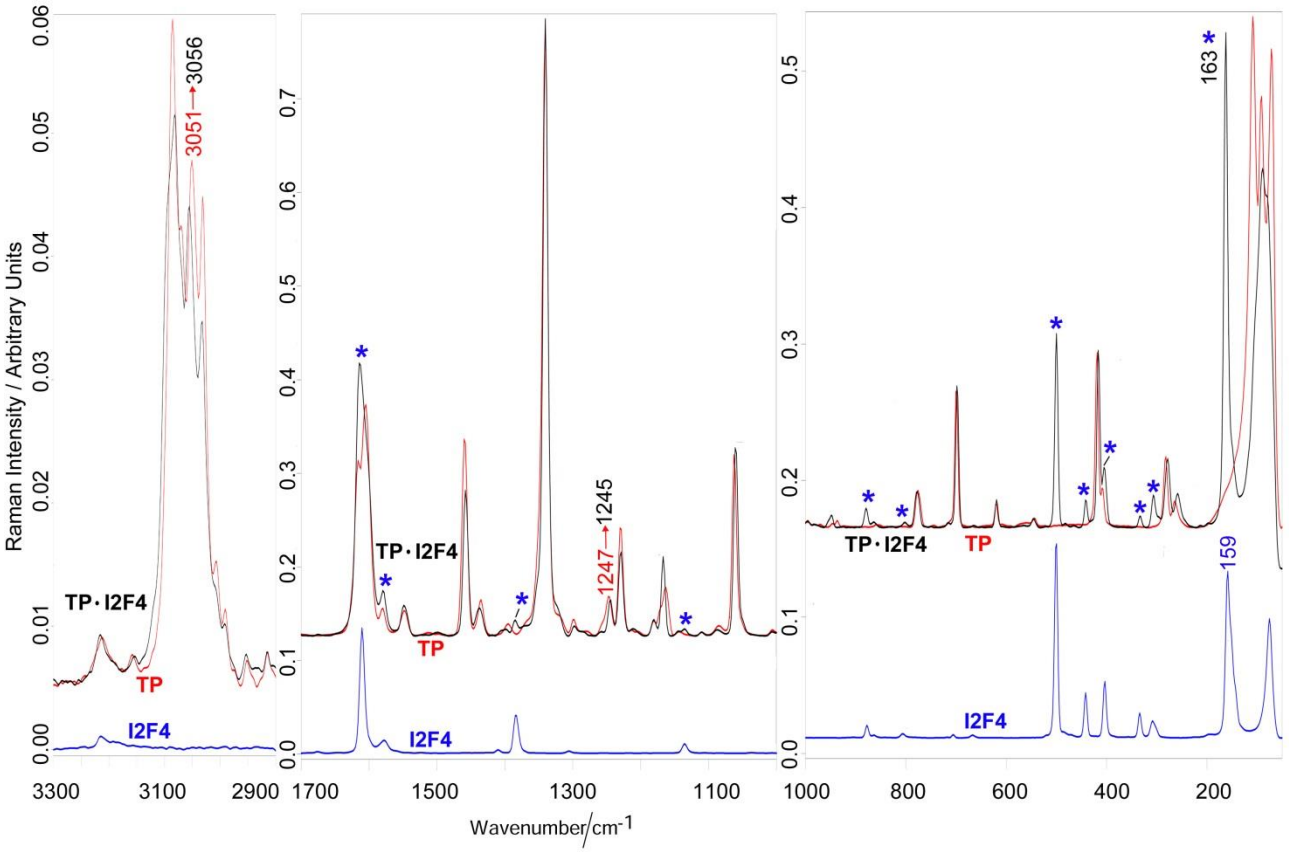

Figure 5. Raman spectra of TP, I2F4 and TP·I2F4 form I. The main bands of the cocrystal having a contribution from I2F4 have been indicated with an asterisk.

By comparing the Raman spectrum of the TP·Br2F4 cocrystal with those of the coformers, i.e. TP and Br2F4 (Figure 6 and Table SI-4 for wavenumbers and assignments),[59-63] trends similar to those above reported for TP·I2F4 form I were observed. Also in this case, the experimental spectrum was not the superposition of the spectra of the single components, and was significantly different from the theoretical one (Figure SI-10), suggesting the occurrence of distinct interactions. The

differences between experimental and theoretical spectra of TP·Br2F4 were observed in the same spectral ranges as for TP·I2F4 form I cocrystal (Figure SI-8).

De Santis et al.[66] have compared the shifts of the I2F4 and Br2F4 bands at 159 and 211 cm^{-1}, respectively, upon halogen bond formation with dipyridyl derivatives; they have reported that the former band shifted to a higher extent than the latter and have ascribed this behavior to the stronger halogen-bonding donating character of I2F4, i.e. to its higher acidity character.

The spectra here reported may be explained accordingly; actually, the I2F4 band at 159 cm^{-1} shifted to 163 cm^{-1} in the TP·I2F4 form I cocrystal (i.e. by 4 cm^{-1}), while the 211 cm^{-1} band shifted to 213 cm^{-1} in the TP·Br2F4 cocrystal (i.e. by 2 cm^{-1}), confirming the above reported trend.

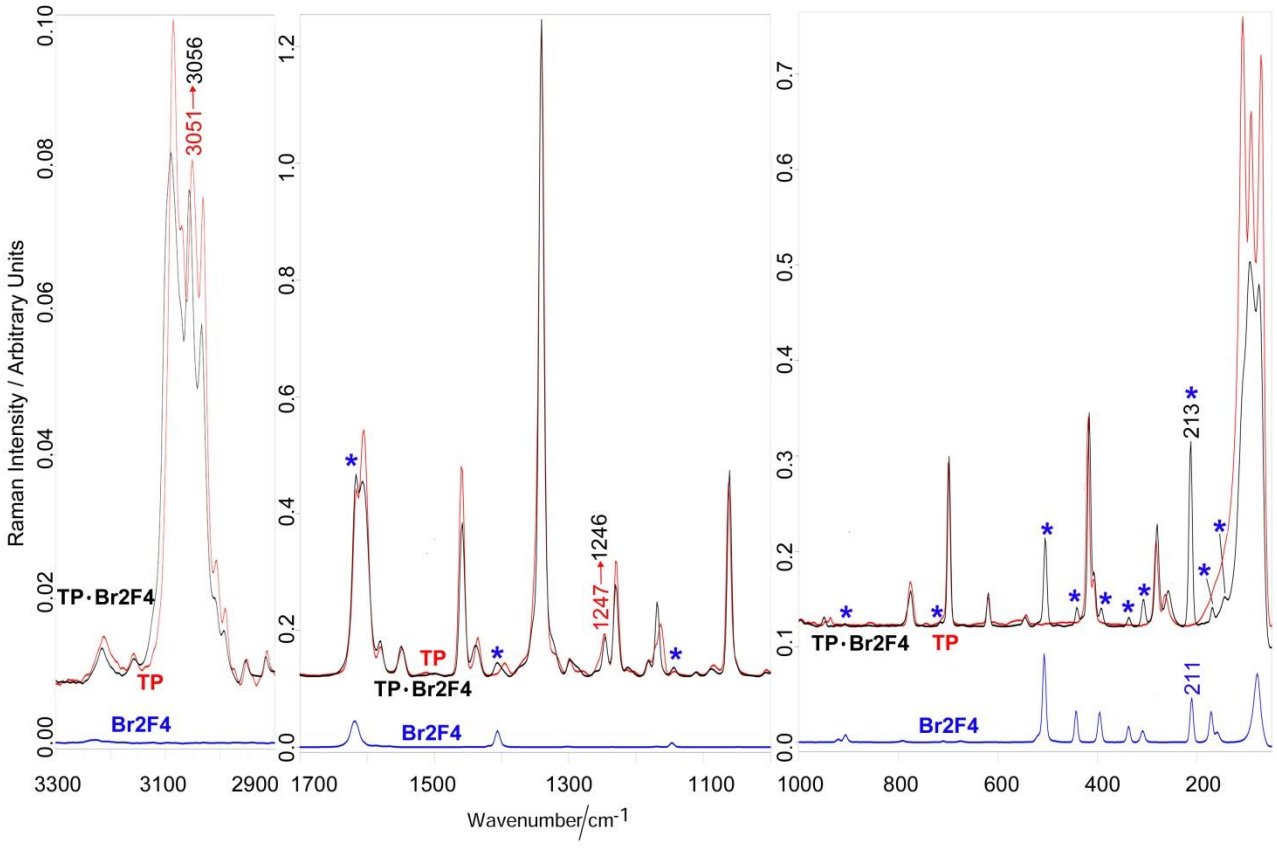

Figure 6. Raman spectra of TP, Br2F4 and TP·Br2F4. The main bands of the cocrystal having a contribution from Br2F4 have been indicated with an asterisk.

Optical spectroscopy

Absorption and emission properties of the stable cocrystals TP·I2F4 form I and TP·Br2F4 have been characterized at room temperature in the solid state and compared to those of bare TP, studied as reference compound. TP·I2F4 luminescence has also been characterized at 77K, to probe the effects of the thermally triggered phase transformation leading to TP·I2F4 form II.

Solid TP showed a bright fluorescence in the 400-500 nm region with a quantum yield of 37%. (Figure 7 and Table 2). The vibronic structure resembled that reported for TP fluorescence in solution,[67,69] but with an overall bathochromic shift of ca. 40 nm. A similar trend has been described for TP spin-coated films and attributed to π-stacking of the planar molecules.[42] The fluorescence decay could be satisfactorily fitted by a bi-exponential function, with a main component in the order of 46 ns (Table 2, Figure SI-11a). TP also exhibited a weak phosphorescence that could be detected only by means of a gated detection (Figure SI-12). It can be noticed that, as well as fluorescence, the observed phosphorescence is largely red-shifted (ca. 90 nm) with respect to that detected for TP in solution at low temperature.[69-71] The phosphorescence decay showed a bi-exponential behavior with lifetimes of ca. 90 ms and 290 ms (Table 2, Figure SI-14a).

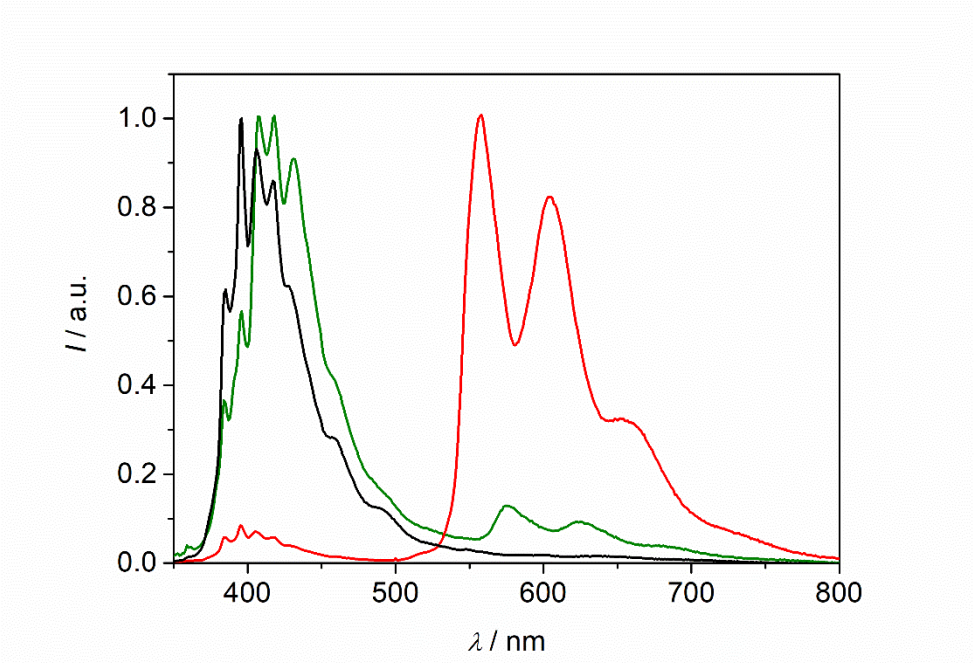

Figure 7. Normalized corrected emission spectra of TP (black), TP·I2F4 form I (red) and TP·Br2F4 (single crystals, olive) in the solid state at room temperature. λ_{exc} = 310 nm.

Table 2. Luminescence data at room temperature.

	Fluorescence			Phosphorescence	
	λ_{max} / nm[a]	ϕ [b]	τ / ns [c]	λ_{max} / nm[d]	τ / ms [e]
TP	385, 396, 406, 418, 427 sh	0.37±0.05	2.6 (30%), 45.5 (70%)	550, 602, 640	90.4 (40%), 287.4 (60%)
TP·I2F4 form I	385, 395, 405, 418, 428 sh	0.36±0.06	2.1 (30%), 44.9 (70%)	558, 604, 656	9.7
TP·Br2F4[f]	384, 396, 408, 418, 431 [384 sh, 408, 416, 428]	- [0.055±0.003]	4.6 (20%), 48.9 (80%) [1.9 (70%), 29.1 (30%)]	580, 632, 686 [576, 624, 684]	208.1 [8.2 (90%), 178.0 (10%)]

[a] From corrected fluorescence spectra. [b] Absolute emission quantum yields, excitation at 320/330 nm. [c] Fluorescence lifetimes, measured by means of a TCSPC apparatus, excitation at 331 nm; mean values from two measurements. Representative decays are shown in Figure SI-11. [d] From corrected phosphorescence spectra acquired with gated detection. [e] Phosphorescence lifetimes, measured by means of a multichannel scaling mode and a Xenon flashlamp as excitation source, excitation at 310 nm; mean values from three to four measurements. Representative decays are shown in Figure SI-14. [f] Data for single crystals; in square brackets data for powder samples.

In contrast to pure TP, the luminescence of cocrystal TP·I2F4 form I was characterized by an intense phosphorescence, being the fluorescence of TP almost completely suppressed (Figure 7). The phosphorescence spectrum, isolated by means of a gated detection, is reported in Figure SI-13. This outcome can be ascribed to the external heavy atom effect produced by the iodine atoms of the co-former which interact with the π system of the TP molecule in the crystal lattice through weak I···π interactions. The phosphorescence lifetime is reduced to ca. 10 ms since, as well as intersystem crossing, the radiative deactivation rate of the triplet state is increased by the presence of the heavy atom. The overall luminescence quantum yield, which is dominated by phosphorescence emission, is 36% (Table 2), i.e. comparable with the fluorescence quantum yield

of the pure TP. This is a remarkable value for organic phosphorescence at room temperature and in aerated conditions. At low temperature TP·I2F4 form II showed a similar behavior, with a weak fluorescence and an intense phosphorescence, the latter characterized by a higher spectral resolution with respect to room temperature (Figure SI-15). The luminescence data at 77 K are summarized in Table SI-5. This result evidences that, even if the structure of form II is characterized by a shift of the I2F4 molecule with respect to the TP plane (Figure 3), the induction of triplet emission from TP is still effective.

Cocrystal TP·Br2F4 showed an almost intermediate behavior, displaying a clear phosphorescence together with a residual fluorescence (Figure 7). For this compound single crystals could be obtained and, interestingly, the luminescence behavior of the crystals was found to be different from that of powder samples (ground crystals). In particular, the relative intensity of phosphorescence *vs* fluorescence was found to be higher for ground crystals (Figure SI-16, see Figure SI-17 for isolated phosphorescence spectra). On the other hand, a notably long triplet excited state lifetime of 208 ms (comparable with that of pure TP) was measured for the crystals, while it reduced to ca. 8 ms (main component) in powder samples (Table 2, Figure SI-14c). Both outcomes can be ascribed to the presence of defects and exciton traps in the ground material which could reduce both fluorescence intensity and phosphorescence lifetime. The luminescence quantum yield, measured for powder samples, was of the order of 6% (Table 2).[§]

It can be noticed that, while the vibronic structure of fluorescence was well comparable among the three compounds (Table 2), the phosphorescence bands displayed a slight (ca. 10 nm) and an important (30-40 nm) red-shift in TP·I2F4 form I and TP·Br2F4, respectively, with respect to bare TP. This indicates a different perturbation of the triplet excited state properties of the TP molecule operated by the two halogen atoms. Moreover, the relative intensity distribution of the vibronic bands was found to be different in the co-crystals, where the most intense peak is at lower energy (558 and 580 nm for TP·I2F4 form I and TP·Br2F4, respectively), compared to TP, where the most

intense band is at 640 nm (Figure SI-12). This results in a visual orange color for the phosphorescence of the cocrystals and in a more reddish color for that of TP (Figure 4 and video in the Supporting Information).

The excitation spectrum of TP collected at 396 nm closely resembles the absorption spectrum of the compound, showing the same fine vibronic structure (Figure SI-18a). Excitation spectra of the two cocrystals collected both in the fluorescence and in the phosphorescence spectral regions reasonably superimpose with the respective absorption spectra (Figure SI-18 b and c), confirming the origin of both singlet and triplet emission in the TP manifold.

CONCLUSIONS

In this work, five new cocrystals made up of the polycyclic aromatic hydrocarbon triphenylene (TP) and halo-perfluorobenzene (XF5 and X2F4, where X = I or Br) co-formers were successfully assembled by π-hole···π, a subclass of π-stacking, and further stabilized by a combination of weak X···π and X···X interactions.

Cocrystals TP·BrF5 and TP·IF5 display disorder of the co-former and are unstable once taken out from the mother liquor, making further spectroscopic characterization unfeasible. Cocrystal TP·I2F4 exists in two different polymorphs as a function of temperature, namely form I and II for RT and LT, respectively. As confirmed by variable temperature SCXRD, transitions between these two phases occur reversibly in a single crystal to single crystal fashion, and, as proved by variable temperature Raman spectroscopy, also in polycrystalline samples.

The luminescence properties of the cocrystals TP·Br2F4, TP·I2F4 form I and TP·I2F4 form II in the solid state were studied and compared with those of pure TP. Interestingly, at a difference with TP which is exclusively fluorescent at room temperature (a weak phosphorescence could be detected only in gated mode), the cocrystals TP·I2F4 form I and TP·Br2F4 were found to be also phosphorescent, but with different properties in their triplet emission depending on the nature of the

involved halogen atom. The higher spin-orbit coupling constant of iodine with respect to bromine (ξ = 5069 and 2460 cm^{-1}, respectively),[72] led to an almost quantitative intersystem crossing in the organic units of TP·I2F4 form I, with the result of a nearly exclusive bright phosphorescence emission. Yet, because of the same process, the triplet excited state lifetime was found to be of the order of 10 ms. The interaction of bromine with the π-system of TP resulted in an effective but not complete quenching of the fluorescence, with the interesting outcome of a phosphorescence lifetime of 208 ms in single crystals. The orange phosphorescence of these crystals, in fact, could be observed by naked eye lasting for ca. 1-2 seconds after ceasing the UV excitation. The luminescence features of TP·I2F4 form II, investigated at 77K, were found to be similar to those observed for form I, indicating that the molecular re-arrangement is not affecting the photophysical properties of the compound.

ASSOCIATED CONTENT

Supporting Information. The Supporting Information is available free of charge via the Internet at http://pubs.acs.org. X-ray crystallographic data for Br2F4. Additional information concerning PXRD, Rietveld Refinement Plots, Raman Spectra, and solid-state luminescence spectroscopy.

X-ray crystallographic data for compound Br2F4, and cocrystal TP·BrF5, TP·Br2F4, TP·IF5, TP·I2F4 form I and TP·I2F4 form II (CIF).

AUTHOR INFORMATION

Corresponding Author

* (F. G.) E-mail: fabrizia.grepioni@unibo.it.

* (B.V.) E-mail: barbara.ventura@isof.cnr.it.

Orcid

Simone d'Agostino 0000-0003-3065-5860

Floriana Spinelli 0000-0002-8445-6173

Paola Taddei 0000-0001-8478-4508

Barbara Ventura 0000-0002-8207-1659

Fabrizia Grepioni: 0000-0003-3895-0979

Author Contributions

The manuscript was written through contributions of all authors. All authors have given approval to the final version of the manuscript.

Funding Sources

Financial support from MIUR, and the University of Bologna is acknowledged. Italian CNR (Project "PHEEL") and MIUR-CNR project "Nanomax" N-CHEM are gratefully acknowledged.

Notes

The authors declare no competing financial interest.

§ The CIE 1931 spectral chromaticity coordinates of the luminescence of TP, TP·I2F4 form I and TP·Br2F4 at room temperature were calculated as (0.17, 0.07), (0.50, 0.47), (0.20, 0.10) respectively. From Figure 4 it can be seen that, under UV irradiation, solid TP is clearly observed as light blue, whereas the difference in color between the two cocrystals is not as evident as the pure luminescence chromaticity coordinates indicate. Indeed, the visual color of the materials under UV irradiation is the results of different factors, i.e. absorption, scattering of the excitation light, emission range and quantum yield.

ABBREVIATIONS

TP, Triphenylene; XF5, halo-pentafluorobenzene; IF5, iodo-pentafluorobenzene; BrF5, bromo-pentafluorobenzene; X2F4, 1,4-dihalo-tetrafluorobenzene; I2F4, 1,4-diiodo-tetrafluorobenzene; Br2F4, 1,4-dibromo-tetrafluorobenzene.

REFERENCES

(1) Forni, A.; Lucenti, E.; Botta, C.; Cariati, E. Metal free room temperature phosphorescence from molecular self-interactions in the solid state. *J. Mater. Chem. C* **2018**, *6* , 4603–4626.

(2) Bolton, O.; Lee, K.; Kim, H. J.; Lin, K. Y.; Kim, Activating efficient phosphorescence from purely organic materials by crystal design. J. *Nat. Chem.* **2011**, *3*, 205–210.

(3) Gao, H. Y.; Zhao, X. R.; Wang, H.; Pang, X.; Jin, W. J. Phosphorescent cocrystals assembled by 1,4-diiodotetrafluorobenzene and fluorene and its heterocyclic analogues based on C-I•••π halogen bonding. *Cryst. Growth Des.* **2012**, *12*, 4377–4387.

(4) Li, D.; Lu, F.; Wang, J.; Hu, W.; Cao, X.-M.; Ma, X.; Tian. H. Amorphous Metal-Free Room-Temperature Phosphorescent Small Molecules with Multicolor Photoluminescence via a Host−Guest and Dual-Emission Strategy. *J. Am. Chem. Soc. 2018*, **140**, 1916-1923.

(5) Yang, J.; Zhen, X.; Wang, B.; Gao, X.; Ren, Z.; Wang, J.; Xie, Y.; Li, J.; Peng, Q.; Pu, K.; Li, Z. The influence of the molecular packing on the room temperature phosphorescence of purely organic luminogens. *Nat. Commun.* **2018**, *9*, 840-850.

(6) Xie, Y.; Ge, Y.; Peng, Q.; Li, C.; Li, Q.; Li, Z. How the Molecular Packing Affects the Room Temperature Phosphorescence in Pure Organic Compounds: Ingenious Molecular Design, Detailed Crystal Analysis, and Rational Theoretical Calculations *Adv. Mater.* **2017**, *29*, 1606829-1606836.

(7) Xu, S.; Chen, R.; Zheng, C.; Huang, W. Excited State Modulation for Organic Afterglow: Materials and Applications. *Adv. Mater.* **2016**, *28*, 9920–9940.

(8) Kabe, R.; Adachi, C. Organic long persistent luminescence. *Nature* **2017**, *550*, 384–387.

(9) DeRosa, C. A.; Samonina-Kosicka, J.; Fan, Z.; Hendargo, H. C.; Weitzel, D. H.; Palmer, G. M.; Fraser, C. L. Oxygen sensing difluoroboron dinaphthoylmethane polylactide. *Macromolecules* **2015**, *48*, 2967–2977.

(10) Al-Attar, H. A.; Monkman, A. P. Room-temperature phosphorescence from films of isolated water-soluble conjugated polymers in hydrogen-bonded matrices. *Adv. Funct. Mater.* **2012**, *22*, 3824–3832.

(11) Hirata, S.; Totani, K.; Zhang, J.; Yamashita, T.; Kaji, H.; Marder, S. R.; Watanabe, T.; Adachi, C. Efficient persistent room temperature phosphorescence in organic amorphous materials under ambient conditions. *Adv. Funct. Mater.* **2013**, *23*, 3386–3397.

(12) Mieno, H.; Kabe, R.; Notsuka, N.; Allendorf, M. D.; Adachi, C. Long-Lived Room-Temperature Phosphorescence of Coronene in Zeolitic Imidazolate Framework ZIF-8. *Adv. Opt. Mater.* **2016**, *4*, 1015–1021.

(13) Wei, J.; Liang, B.; Duan, R.; Cheng, Z.; Li, C.; Zhou, T.; Yi, Y.; Wang, Y. Induction of Strong Long-Lived Room-Temperature Phosphorescence of N-Phenyl-2-naphthylamine Molecules by Confinement in a Crystalline Dibromobiphenyl Matrix. *Angew. Chem.Int. Ed.* **2016**, *128*, 15818-15822.

(14) Deng, Y.; Zhao, D.; Chen, X.; Wang, F.; Song, H.; Shen, D. Long lifetime pure organic phosphorescence based on water soluble carbon dots. *Chem. Commun.* **2013**, *49*, 5751–5753.

(15) Bian, L.; Shi, H.; Wang, X.; Ling, K.; Ma, H.; Li, M.; Cheng, Z.; Ma, C.; Cai, S.; Wu, Q.; Gan, N.; Xu, X.; An, Z.; Huang, W. Simultaneously Enhancing Efficiency and Lifetime of Ultralong Organic Phosphorescence Materials by Molecular Self-Assembly. *J. Am. Chem. Soc.* **2018**, *140*, 10734-10739.

(16) Sun, C.; Ran, X.; Wang, X.; Cheng, Z.; Wu, Q.; Cai, S.; Gu, L.; Gan, N.; Shi, H.; An, Z.; Shi, H.; Huang, W. Twisted Molecular Structure on Tuning Ultralong Organic Phosphorescence. *J. Phys. Chem. Lett.* **2018**, *9*, 335–339.

(17) Cai, S.; Shi, H.; Zhang, Z.; Wang, X.; Ma, H.; Gan, N.; Wu, Q.; Cheng, Z.; Ling, K.; Gu, M.; Ma, C.; Gu, L.; An, Z.; Huang, W. Hydrogen-Bonded Organic Aromatic Frameworks for Ultralong Phosphorescence by Intralayer π–π Interactions. *Angew. Chemie - Int. Ed.* **2018**, *57*, 4005–4009.

(18) Zhang, G.; Palmer, G. M.; Dewhirst, M. W.; Fraser, C. L. A dual-emissive-materials design concept enables tumour hypoxia imaging. *Nat. Mater.* **2009**, *8*, 747–751.

(19) Yoshihara, T.; Yamaguchi, Y.; Hosaka, M.; Takeuchi, T.; Tobita, S. Ratiometric molecular sensor for monitoring oxygen levels in living cells. *Angew. Chemie - Int. Ed.* **2012**, *51*, 4148–4151.

(20) Koch, M.; Perumal, K.; Blacque, O.; Garg, J. A.; Saiganesh, R.; Kabilan, S.; Balasubramanian, K. K.; Venkatesan, K. Metal-free triplet phosphors with high emission efficiency and high tunability. *Angew. Chemie - Int. Ed.* **2014**, *53*, 6378–6382.

(21) Braga, D.; Grepioni, F.; Maini, L.; D'Agostino, S. Making crystals with a purpose; A journey in crystal engineering at the University of Bologna. *IUCrJ* **2017**, *4*, 369-379.

(22) Braga, D.; Grepioni, F.; Maini, L.; d'Agostino, S. From Solid-State Structure and Dynamics to Crystal Engineering. *Eur. J. Inorg. Chem.* **2018**, 3597–3605.

(23) Desiraju, G. R. Crystal engineering: From molecule to crystal. *J. Am. Chem. Soc.* **2013**, *135*, 9952–9967.

(24) Christopherson, J. C.; Topić, F.; Barrett, C. J.; Friščić, T. Halogen-Bonded Cocrystals as Optical Materials: Next-Generation Control over Light-Matter Interactions. *Cryst. Growth Des.* **2018**, *18*, 1245–1259.

(25) Wang, Y.; Zhu, W.; Du, W.; Liu, X.; Zhang, X.; Dong, H.; Hu, W. Cocrystals Strategy towards Materials for Near-Infrared Photothermal Conversion and Imaging. *Angew. Chemie - Int. Ed.* **2018**, *57* , 3963–3967.

(26) Li, Z. Z.; Liang, F.; Zhuo, M. P.; Shi, Y. L.; Wang, X. D.; Liao, L. S. White-Emissive Self-Assembled Organic Microcrystals. *Small* **2017**, *13*, 1–6.

(27) Carletta, A.; Buol, X.; Leyssens, T.; Champagne, B.; Wouters, J. Polymorphic and Isomorphic Cocrystals of a N-Salicylidene-3-aminopyridine with Dicarboxylic Acids: Tuning of Solid-State Photo- and Thermochromism. *J. Phys. Chem. C* **2016**, *120*, 10001–10008.

(28) Carletta, A.; Spinelli, F.; D'Agostino, S.; Ventura, B.; Chierotti, M. R.; Gobetto, R.; Wouters, J.; Grepioni, F. Halogen-Bond Effects on the Thermo- and Photochromic Behaviour of Anil-Based Molecular Co-crystals. *Chem. - A Eur. J.* **2017**, *23*, 5317–5329.

(29) Hutchins, K. M.; Dutta, S.; Loren, B. P.; Macgillivray, L. R. Co-crystals of a salicylideneaniline: Photochromism involving planar dihedral angles. *Chem. Mater.* **2014**, *26*, 3042–3044.

(30) D'Agostino, S.; Grepioni, F.; Braga, D.; Moreschi, D.; Fattori, V.; Delchiaro, F.; Di Motta, S.; Negri, F. Exciton coupling in molecular salts of 2-(1,8-naphthalimido)ethanoic acid and cyclic amines: Modulation of the solid-state luminescence. *CrystEngComm* **2013**, *15*, 10470–10480.

(31) Yan, D.; Delori, A.; Lloyd, G. O.; Friščić, T.; Day, G. M.; Jones, W.; Lu, J.; Wei, M.; Evans, D. G.; Duan, X. A cocrystal strategy to tune the luminescent properties of stilbene-type organic solid-state materials. *Angew. Chemie - Int. Ed.* **2011**, *50*, 12483–12486.

(32) Anthony, S. P. Organic solid-state fluorescence: Strategies for generating switchable and tunable fluorescent materials. *Chempluschem* **2012**, *77*, 518–531.

(33) Grepioni, F.; D'Agostino, S.; Braga, D.; Bertocco, A.; Catalano, L.; Ventura, B. Fluorescent crystals and co-crystals of 1,8-naphthalimide derivatives: synthesis, structure determination and photophysical characterization. *J. Mater. Chem. C* **2015**, *3*, 9425–9434.

(34) Khan, A.; Wang, M.; Usman, R.; Sun, H.; Du, M.; Xu, C. Molecular Marriage via Charge Transfer Interaction in Organic Charge Transfer Co-Crystals toward Solid-State Fluorescence Modulation. *Cryst. Growth Des.* **2017**, *17*, 1251–1257.

(35) Sun, H.; Wang, M.; Khan, A.; Shan, Y.; Zhao, K.; Usman, R.; Xu, C. Co-crystals with Delayed Fluorescence Assembled by 1,4-Diiodotetrafluorobenzene and Polycyclic Aromatic Compounds via

Halogen Bonds. *ChemistrySelect* **2017**, *2*, 6323–6330.

(36) Pashazadeh, R.; Pander, P.; Lazauskas, A.; Dias, F. B.; Grazulevicius, J. V. Multicolor Luminescence Switching and Controllable Thermally Activated Delayed Fluorescence Turn on/Turn off in Carbazole-Quinoxaline-Carbazole Triads. *J. Phys. Chem. Lett.* **2018**, *9*, 1172–1177.

(37) Pang, X.; Wang, H.; Wang, W.; Jin, W. J. Phosphorescent π-Hole···π Bonding Cocrystals of Pyrene with Halo-perfluorobenzenes (F, Cl, Br, I). *Cryst. Growth Des.* **2015**, *15*, 4944–4945.

(38) Gao, H. Y.; Shen, Q. J.; Zhao, X. R.; Yan, X. Q.; Pang, X.; Jin, W. J. Phosphorescent co-crystal assembled by 1,4-diiodotetrafluorobenzene with carbazole based on C-I···π halogen bonding. *J. Mater. Chem.* **2012**, *22*, 5336–5343.

(39) d'Agostino, S.; Grepioni, F.; Braga, D.; Ventura, B. Tipping the balance with the aid of stoichiometry: Room temperature phosphorescence versus fluorescence in organic cocrystals. *Cryst. Growth Des.* **2015**, *15*, 2039–2045.

(40) Ventura, B.; Bertocco, A.; Braga, D.; Catalano, L.; D'Agostino, S.; Grepioni, F.; Taddei, P. Luminescence properties of 1,8-naphthalimide derivatives in solution, in their crystals, and in co-crystals: Toward room-temperature phosphorescence from organic materials. *J. Phys. Chem. C* **2014**, *118*, 18646–18658.

(41) Zhu, Q.; Gao, Y. J.; Gao, H. Y.; Jin, W. J. Effect of N-methyl and ethyl on phosphorescence of carbazole in cocrystals assembled by C-I···π halogen bond, π-hole···π bond and other interactions using 1,4-diiodotetrafluorobenzene as donor. *J. Photochem. Photobiol. A Chem.* **2014**, *289*, 31–38.

(42) Li, L.; Wu, W. X.; Liu, Z. F.; Jin, W. J. Effect of geometry factors on the priority of σ-hole···π and π-hole···π bond in phosphorescent cocrystals formed by pyrene or phenanthrene and trihaloperfluorobenzenes. *New J. Chem.* **2018**, *42*, 10633-10641.

(43) Lapadula, G.; Judaš, N.; Friščić, T. A three-component modular strategy to extend and link coordination complexes by using halogen bonds to O, S and π acceptors. *Chem. - A Eur. J.* **2010**, *16*,

7400–7403.

(44) Lipstman, S.; Muniappan, S.; Goldberg, I. Supramolecular reactivity of porphyrins with mixed iodophenyl and pyridyl meso-substituents. *Cryst. Growth Des.* **2008**, *8*, 1682–1688.

(45) Wang, J.; Gu, X.; Ma, H.; Peng, Q.; Huang, X.; Zheng, X.; Sung, S. H. P.; Shan, G.; Lam, J. W.Y.; Shuai, Z.; Tang, B. Z. A facile strategy for realizing room temperature phosphorescence and single molecule white light emission. *Nat. Commun.* **2018**, *9*, 2963-2972.

(46) Haneline, M. R.; Tsunoda, M.; Gabbai, π-complexation of biphenyl, naphthalene, and triphenylene to trimeric perfluoro-ortho-phenylene mercury. Formation of extended binary stacks with unusual luminescent properties. F. P. *J. Am. Chem. Soc.* **2002**, *124*, 3737–3742.

(47) Unterleitner, F. C.; Hormats, E. I. Rates of decay of phosphorescence from triphenylene in acrylic polymers. *J. Phys. Chem.* **1965**, *69*, 2516–2520.

(48) Levell, J. W.; Ruseckas, A.; Henry, J. B.; Wang, Y.; Stretton, A. D.; Mount, A. R.; Galow, T. H.; Samuel, I. D. W. Fluorescence enhancement by symmetry breaking in a twisted triphenylene derivative. *J. Phys. Chem. A* **2010**, *114*, 13291–13295.

(49) Pawley, G. S.; Mackenzie, G. A.; Dietrich, O. W. Acta Acta Cryst. 1977, A33, 142-145.

(50) Sheldrick, G. M. SHELX97, *Program for Crystal Structure Determination*; University of Göttingen: Göttingen, Germany, **1997**.

(51) Macrae, C. F.; Bruno, I. J.; Chisholm, J. A.; Edgington, P. R.; McCabe, P.; Pidcock, E.; Rodriguez-Monge, L.; Taylor, R.; Van De Streek, J.; Wood, P. A. New features for the visualization and investigation of crystal structures. *J. Appl. Crystallogr.* **2008**, *41*, 466–470.

(52) Cohelo, A. *TOPAS-Academic*; Coelho Software: Brisbane, Australia, **2007**.

(53) Ishida, H.; Tobita, S.; Hasegawa, Y.; Katoh, R.; Nozaki, K. Recent advances in instrumentation for absolute emission quantum yield measurements. *Coord. Chem. Rev.* **2010**, *254*, 2449–2458.

(54) Metrangolo, P.; Resnati, G. Type II halogen···halogen contacts are halogen bonds. *IUCrJ* **2014**, *1*, 5–7.

(55) Desiraju, G. R.; Parthasarathy, R. The Nature of Halogen•••Halogen Interactions: Are Short Halogen Contacts Due to Specific Attractive Forces or Due to Close Packing of Nonspherical Atoms? *J. Am. Chem. Soc.* **1989**, *111*, 8725–8726.

(56) Ovens, J. S.; Leznoff, D. B. Probing halogen···halogen interactions *via* thermal expansion analysis. *CrystEngComm* **2018**, *20*, 1769–1773.

(57) Navon, O.; Bernstein, J.; Khodorkovsky, V. Ladders, and Two-Dimensional Sheets with Halogen ··· Halogen and Halogen ··· Hydrogen Interactions. *Angew. Chem., Int. Ed.* **1997**, *36*, 601–603.

(58) Carletta, A.; Meinguet, C.; Wouters, J.; Tilborg, A. Solid-state investigation of polymorphism and tautomerism of phenylthiazole-thione: A combined crystallographic, calorimetric, and theoretical survey. *Cryst. Growth Des.* **2015**, *15*, 2461–2473.

(59) Colangeli, L.; Mennella, V.; Baratta, G. A.; Bussoletti, E.; Strazzulla, G. Raman and infrared spectra of polycyclic aromatic hydrocarbon molecules of possible astrophysical interest. *Astrophys. J.* **1992**, *396*, 369–377.

(60) Zhao, X. M.; Zhong, G. H.; Zhang, J.; Huang, Q. W.; Goncharov, A. F.; Lin, H. Q.; Chen, X. J. Combined experimental and computational study of high-pressure behavior of triphenylene. *Sci. Rep.* **2016**, *6*, 1–10.

(61) López-Tocón, I.; Otero, J. C.; Arenas, J. F.; García-Ramos, J. V.; Sánchez-Cortés, S. Trace detection of triphenylene by surface enhanced raman spectroscopy using functionalized silver nanoparticles with bis-acridinium lucigenine. *Langmuir* **2010**, *26*, 6977–6981.

(62) Hanson, G. R.; Jensen, P.; McMurtrie, J.; Rintoul, L.; Micallef, A. S. Halogen bonding between an isoindoline nitroxide and 1,4- diiodotetrafluorobenzene: New tools and tectons for self-assembling organic spin systems. *Chem. - A Eur. J.* **2009**, *15*, 4156–4164.

(63) Green, J.H.S.; Harrison, D.J. Vibrational spectra of benzene derivatives – XVIII dihalogenotetrafluorobenzenes. Spectrochim. *Acta Part A* **1977**,193–197.

(64) Shen, Q. J.; Wei, H. Q.; Zou, W. S.; Sun, H. L.; Jin, W. J. Cocrystals assembled by pyrene and 1,2- or 1,4-diiodotetrafluorobenzenes and their phosphorescent behaviors modulated by local molecular environment. *CrystEngComm* **2012**, *14*, 1010–1015.

(65) Shen, Q. J.; Pang, X.; Zhao, X. R.; Gao, H. Y.; Sun, H. L.; Jin, W. J. Phosphorescent cocrystals constructed by 1,4-diiodotetrafluorobenzene and polyaromatic hydrocarbons based on C-I···π halogen bonding and other assisting weak interactions. *CrystEngComm* **2012**, *14*, 5027–5034.

(66) De Santis, A.; Forni, A.; Liantonio, R.; Metrangolo, P.; Pilati, T.; Resnati, G. N···Br halogen bonding: One-dimensional infinite chains through the self-assembly of dibromotetrafluorobenzenes with dipyridyl derivatives. *Chem. - A Eur. J.* **2003**, *9*, 3974–3983.

(67) Nakajima, A. Solvent effect on the vibrational structures of the fluorescence spectra of coronene and triphenylene. *J. Lumin.* **1974**, *8*, 266–269.

(68) Sasson, R.; Braitbart, O.; Weinreb, A. On the emission spectrum of triphenylene. *J. Lumin.* **1988**, *39*, 223-225.

(69) Nobuyuki Nishi , Kazunori Matsui , Minoru Kinoshita & Jiro Higuchi Study on the triplet state of triphenylene by microwave induced delayed phosphorescence and T←S excitation spectroscopy MOLECULAR PHYSICS, 1979, VOL. 38, NO. 1, 1-24;

(70) Offen, H. W.; Hein, D. E. Environmental Effects on Phosphorescence. VI. Matrix Site Effects for Triphenylene. *J. Chem. Phys.* **1969**, *50*, 5274-5278.

(71) Vikesland, J.P.; Wilkinson F. Quenching of Triphenylene Phosphorescence in Poly-(methylmethacrylate) at 77 K by Ferrocene and Ruthenocene. *Faraday Trans.* **1977**,*73*, 1082-1093

(72) Montalti, M.; Credi, A.; Prodi, L.; Gandolfi, M. T. *Handbook of Photochemistry, Third Edition*; CRC-Taylor & Francis, Boca Raton, **2006**.

For Table of Contents Use Only

Ultralong Organic Phosphorescence in the Solid State: the Case of Triphenylene Cocrystals with Halo- and Dihalo-penta/tetrafluorobenzene

Simone d'Agostino, Floriana Spinelli, Paola Taddei, Barbara Ventura and Fabrizia Grepioni

TOC graphic

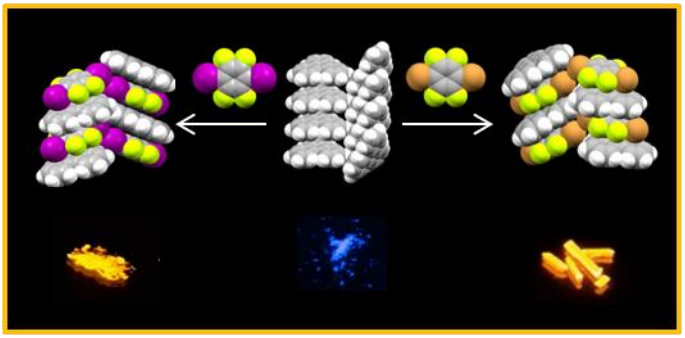

SYNOPSIS

Here we report on the solid state preparation and characterization of a series of cocrystals with general formula TP·XF5 and TP·X2F4, where TP = triphenylene and XF5, X2F4 = halo-perfluorobenzenes (X = I or Br). In contrast to the parent compound TP, which shows intense fluorescence and faint phosphorescence in the solid state, cocrystals TP·X2F4 exhibit intense RT orange phosphorescence emission. In the case of TP·Br2F4, the phosphorescence lifetime of 208 ms makes it classifiable as an UOP compound.